

Cluster Analysis of the Dermal Permeability and Stratum Corneum/Solvent Partitioning of Ten Chemicals in Twenty-Four Chemical Mixtures in Porcine Skin

D. van der Merwe J.E. Riviere

Center for Chemical Toxicology Research and Pharmacokinetics, North Carolina State University, Raleigh, N.C., USA

Key Words

Hierarchical clustering · K-means clustering · Skin permeability · Stratum corneum partitioning

Abstract

Assumptions based on absorption from single solvent systems may be inappropriate for risk assessment when chemical mixtures are involved. We used K-means and hierarchical cluster analyses to identify clusters in stratum corneum partitioning and porcine skin permeability datasets that are distinct from each other based on mathematical indices of similarity and dissimilarity. Twenty-four solvent systems consisting of combinations of water, ethanol, propylene glycol, methyl nicotinate and sodium lauryl sulfate were used with 10 solutes, including phenol, *p*-nitrophenol, pentachlorophenol, methyl parathion, ethyl parathion, chlorpyrifos, fenthion, simazine, atrazine and propazine. Identifying the relationships between solvent systems that have similar effects on dermal absorption formed the bases for hypotheses generation. The determining influence of solvent polarity on the partitioning data structure supported the hypothesis that solvent polarity drives the partitioning of non-polar solutes. Solvent polarity could not be used to predict permeability because solvent effects on diffusiv-

ity masked the effects of partitioning on permeability. The consistent influence of the inclusion of propylene glycol in the solvent system supports the hypothesis that over-saturation due to solvent evaporation has a marked effect on permeability. These results demonstrated the potential of using cluster analysis of large datasets to identify consistent solvent and chemical mixture effects.

Copyright © 2006 S. Karger AG, Basel

Introduction

The absorption of small, relatively non-polar solutes through mammalian skin occurs predominantly by partitioning into the stratum corneum lipids, moving through the stratum corneum lipid matrix, the viable epidermis and partitioning into blood in the dermal blood vessels. The stratum corneum forms the primary barrier to dermal absorption [1]. The rate and extent of solute flux across the skin is related to the exposure area, the extent of solute partitioning into the skin, the ease of solute movement through the skin, the solute concentration gradient and the pathway length. The initial concentration in the solvent, the rate of solute movement into the skin and the effects of solvent and solute evaporation into the

atmosphere determine the concentration gradient. Evaporation, rate of movement in the skin and solvent/skin partitioning are dependent on the solute concentration gradient and the net influence of all the intermolecular forces acting in the system. The forces include H-bonding, covalent bonding, London dispersion forces and charge-charge interactions. They are dependent on the chemical-physical properties of the solute, the solvent system and the skin. If the physical chemical properties of the skin remain relatively constant, although it should be noted that it could change due to the effects of solutes, it is reasonable to hypothesize that dermal absorption is correlated with quantifiable molecular descriptors of the solute. This approach has been used with some success to develop models of dermal absorption of single solutes from single solvents [2]. However, such models are inadequate when multiple solvent systems and chemical mixtures are considered due to the vast number of different chemical environments that can be encountered and the altered influence of particular descriptors when the physical-chemical environment of the solvent system is changed. This was demonstrated recently using a hybrid quantitative structure permeation relationship model that incorporated a mixture factor, based on the physical-chemical properties of the solvent, to improve permeability predictions from chemical mixtures [3]. Complex chemical mixtures are the norm in situations of dermal exposure to potentially harmful chemicals. Assumptions based on absorption from single solvent systems may be inappropriate for risk assessment when chemical mixtures are involved. Large datasets of dermal absorption from a range of solvent systems could potentially indicate consistent solvent effects associated with types of solvent systems, which could reduce uncertainty when predicting dermal absorption.

We used dermatomed porcine skin in flow-through cells to study solvent and chemical mixture effects on dermal absorption. It is a convenient and relatively high throughput in vitro model for the most significant dermal barrier, the stratum corneum, but does not include the effects of dermal blood flow. Surface area, skin thickness and environmental conditions can be controlled to allow solvent and chemical mixture effects to be isolated from random experimental variability. Hierarchical and K-means clustering were used to identify data structure in a quantifiable manner. Cluster analysis is useful where large numbers of treatments and apparently similar numerical data points prevent intuitive identification of data structure. Cluster analyses identify clusters in a dataset that are distinct from each other based on mathe-

matical indices of similarity and dissimilarity. Identifying the relationships between treatments that have similar effects on dermal absorption could form the bases for hypotheses generation.

Methods

Chemicals

Atrazine-ring-UL-¹⁴C (specific activity = 15.1 mCi/mmol, purity = 98.1%), methyl parathion-ring-UL-¹⁴C (specific activity = 13.8 mCi/mmol, purity = 99.5%), 4-nitrophenol-UL-¹⁴C (specific activity = 6.4 mCi/mmol, purity = 99.6%), parathion-ring-UL-¹⁴C (specific activity = 9.2 mCi/mmol, purity = 97.1%), pentachlorophenol-ring-UL-¹⁴C (specific activity = 11.9 mCi/mmol, purity = 98.0%), phenol-UL-¹⁴C (specific activity = 9.0 mCi/mmol, purity = 98.5%) and simazine-ring-UL-¹⁴C (specific activity = 15.5 mCi/mmol, purity = 99.0%) were obtained from Sigma Chemical Co. (St. Louis, Mo.). Chlorpyrifos[pyridine-2,6-¹⁴C] (specific activity = 32 mCi/mmol, purity = 99.0%), fenthion-ring-UL-¹⁴C (specific activity = 55 mCi/mmol, purity = 98.5%) and propazine-ring-UL-¹⁴C (specific activity = 15 mCi/mmol, purity = 96.6%) were obtained from American Radiolabeled Chemicals, Inc. (St. Louis, Mo.). Absolute (200 proof) ethanol was obtained from Aaper Alcohol and Chemical Co. (Shelbville, Ky.). Propylene glycol (purity = 99%) was obtained from Sigma Chemical Co. Sodium lauryl sulfate (SLS) (99%, GC grade) was obtained from Fisher Scientific (Pittsburgh, Pa.). Methyl nicotinic acid (MNA) (purity = 99%) was obtained from Sigma Chemical Co. Double distilled water was obtained from our in-house still. Bovine serum albumin (Fract V; cold alcohol precipitated), NaCl (certified ACS), KCl (certified ACS), CaCl (certified ACS; anhydrous), KH₂PO₄ (certified ACS), MgSO₄·7H₂O (certified ACS), NaHCO₃ (certified ACS) and dextrose (certified ACS; anhydrous) were obtained from Fisher Scientific. Amikacin (250 µg/ml) was obtained from Abbott Labs (Chicago, Ill.). Heparin (1,000 units/ml) was obtained from Elkins Sinn (Cherry Hill, N.Y.). Penicillin G sodium (250,000 units/ml) was obtained from Pfizer Inc. (New York, N.Y.).

The receptor solution consisted of 13.78 g NaCl, 0.71 g KCl, 0.56 g CaCl, 0.32 g KH₂PO₄, 0.58 g MgSO₄·7H₂O, 5.50 g NaHCO₃, 2.40 g dextrose, 90.0 g bovine serum albumin, 0.25 ml amikacin, 10 ml heparin and 0.1 ml penicillin G sodium and was made up to 2 liters with glass-distilled water. Water, ethanol and propylene glycol were mixed with each other at 1:1 ratios (by volume). SLS could not be dissolved directly into ethanol and propylene glycol. A 40% mass/mass aqueous solution was added to the solvents/solvent mixtures at a ratio of 25% v/v. The proportional compositions of solvent systems (by mass) are summarized in table 1.

Stratum Corneum/Solvent Partitioning

Stratum corneum/solvent partition coefficients were estimated according to published methods [4]. In short, the stratum corneum of female weanling Yorkshire pigs was removed after heat treatment and immersed in 0.25% trypsin (Sigma Chemical Co.) for 24 h, dried in a Fisherbrand Desiccator Cabinet (Fisher Scientific) with DrieriteTM anhydrous calcium sulfate (WA Hammond Drierite Company, Xenia, Ohio). Stratum corneum samples were weighed (5–8 mg per sample) using a Mettler AE 200 scale (Mettler Toledo,

Table 1. Solvent system numbers, names, proportional mass compositions and polarity indexes

Number	Solvent system	Ethanol %	Water %	PG %	MNA %	SLS %	Polarity index
1	Ethanol	100	0	0	0	0	1.070
2	Ethanol + MNA	99.84	0	0	0.16	0	1.072
3	Ethanol + SLS	62.76	26.60	0	0	10.64	0.989
4	Ethanol + MNA + SLS	62.67	26.56	0	0.14	10.63	0.990
5	Ethanol + water	43.30	56.70	0	0	0	0.463
6	Ethanol + water + MNA	43.92	55.94	0	0.14	0	0.473
7	Ethanol + water + SLS	39.55	50.38	0	0	10.08	0.723
8	Ethanol + water + MNA + SLS	39.50	50.31	0	0.13	10.06	0.725
9	Water	0	100	0	0	0	0
10	Water + MNA	0	99.87	0	0.13	0	0.003
11	Water + SLS	0	90.91	0	0	9.09	0.271
12	Water + MNA + SLS	0	90.47	0	0.12	9.41	0.283
13	Ethanol + PG	43.11	0	56.89	0	0	0.723
14	Ethanol + PG + MNA	43.05	0	56.81	0.14	0	0.725
15	Ethanol + PG + SLS	28.46	24.22	37.63	0	9.69	0.766
16	Ethanol + PG + MNA + SLS	28.43	24.19	37.59	0.12	9.67	0.768
17	PG	0	0	100	0	0	0.460
18	PG + MNA	0	0	99.87	0.13	0	0.462
19	PG + SLS	0	22.18	68.95	0	8.87	0.582
20	PG + MNA + SLS	0	22.96	67.74	0.12	9.18	0.588
21	Water + PG	0	49.11	50.89	0	0	0.234
22	Water + PG + MNA	0	49.05	50.82	0.13	0	0.237
23	Water + PG + SLS	0	44.72	46.34	0	8.94	0.480
24	Water + PG + MNA + SLS	0	44.51	46.12	0.12	9.26	0.491

PG = Propylene glycol.

Columbus, Ohio), placed in vials with 3 ml solvent and 100 μg radio-labeled compound ($n = 5$) and capped. Solvent samples (250 μl) were removed after 24 h. Compound concentrations were estimated by direct radiolabel counts using Ecolume (ICN Costa Mesa, Calif.) and a Packard Model 1900TR Liquid Scintillation Counter (Packard Chemical Co., Downers Grove, Ill.). The stratum corneum was dried by gentle blotting on KimwipeTM and combusted in a Packard Model 306 Tissue Oxidizer (Packard Chemical Co.) for scintillation counting. For partition coefficient determinations, radioactivity content in the vehicle mixture and stratum corneum were normalized to 1,000 mg vehicle (C_{vehicle}) and 1,000 mg stratum corneum ($C_{\text{stratum corneum}}$), respectively. The log stratum corneum/vehicle partition coefficient was determined from the equation: $\log P = \log C_{\text{stratum corneum}}/C_{\text{vehicle}}$.

Permeability

A flow-through diffusion cell system, incorporating 500 μm dermatomed porcine skin disks from the backs of female weanling Yorkshire pigs as diffusion barriers, was used according to the methodology of Chang and Riviere [5] as adapted from Bronaugh and Stewart [6]. The solvent volume was 20 μl . Doses (followed by standard errors in brackets) were: 10.34 $\mu\text{g}/\text{cm}^2$ (0.24) for methyl parathion, 15.15 $\mu\text{g}/\text{cm}^2$ (0.33) for ethyl parathion, 5.69 $\mu\text{g}/\text{cm}^2$ (0.13) for chlorpyrifos, 5.93 $\mu\text{g}/\text{cm}^2$ (0.06) for fenthion, 7.89 $\mu\text{g}/\text{cm}^2$ (0.06) for phenol, 13.71 $\mu\text{g}/\text{cm}^2$ (0.05) for *p*-nitrophenol,

13.43 $\mu\text{g}/\text{cm}^2$ (0.16) for pentachlorophenol, 8.61 $\mu\text{g}/\text{cm}^2$ (0.03) for atrazine, 6.87 $\mu\text{g}/\text{cm}^2$ (0.08) for simazine and 10.69 $\mu\text{g}/\text{cm}^2$ (0.14) for propazine. Perfusate ($n = 4$ or 5) was collected at 15-min intervals for the first 2 h and at 1-hour intervals thereafter up to 8 h. The radiolabel in the perfusate was determined by liquid scintillation as described above. The receptor fluid was assumed to be an infinite sink due to constant receptor fluid flow out of the diffusion cell. Permeability (cm/h) was estimated by dividing the slope of the steady-state portion of the cumulative mass absorbed/time curve with the concentration in the donor solvent.

Polarity Index

A polarity index was used to quantify the relative polarity of the various solvent systems. This allowed relative solvent system polarity to be used in quantitative comparisons. A solvent system polarity index was created by summing the products of the log *P* values of each component and their proportional contributions to the total mass of the solvent system (mass of component/mass of total solvent system). The summed products were then normalized by adding the absolute value of the lowest number to each summed product. This resulted in an index where the lowest index value was zero and the increased index value represented increased non-polarity. log *P* values were obtained from the Syracuse Research Corporation online database and are: -0.31 for ethanol, -1.38 for water, -0.92 for propylene glycol, 0.83 for MNA and 1.60 for SLS. log *P* values

Table 2. Solute partitioning (log P) followed by standard errors in brackets

	Phenol (log P)	PNP (log P)	PCP (log P)	Mparathion (log P)	Parathion (log p)	Chlorpyrifos (log P)	Fenthion (log P)	Simazine (log P)	Atrazine (log P)	Propazine (log P)
Ethanol	0.56 (0.05)	0.63 (0.06)	0.90 (0.09)	0.73 (0.05)	0.98 (0.04)	0.85 (0.07)	0.69 (0.06)	0.77 (0.01)	0.78 (0.05)	0.80 (0.06)
Ethanol+MNA	0.55 (0.10)	0.59 (0.09)	1.06 (0.03)	0.95 (0.09)	1.11 (0.08)	0.83 (0.06)	0.81 (0.04)	0.63 (0.06)	0.73 (0.08)	0.58 (0.06)
Ethanol+SLS	0.50 (0.04)	0.66 (0.07)	1.19 (0.14)	0.77 (0.04)	0.76 (0.09)	0.79 (0.03)	0.76 (0.03)	0.93 (0.03)	0.60 (0.10)	0.74 (0.05)
Ethanol+MNA+SLS	0.51 (0.03)	0.54 (0.08)	0.97 (0.02)	0.95 (0.05)	0.81 (0.06)	0.92 (0.07)	0.65 (0.09)	0.92 (0.03)	0.79 (0.03)	0.75 (0.10)
Ethanol+water	0.75 (0.05)	0.69 (0.01)	1.60 (0.04)	0.99 (0.05)	0.96 (0.06)	1.61 (0.03)	1.01 (0.05)	1.25 (0.02)	0.67 (0.05)	0.77 (0.10)
Ethanol+water+MNA	0.77 (0.02)	0.72 (0.02)	1.48 (0.04)	1.10 (0.08)	0.91 (0.03)	1.34 (0.06)	1.06 (0.06)	1.17 (0.03)	0.61 (0.03)	0.76 (0.04)
Ethanol+water+SLS	0.59 (0.04)	0.48 (0.04)	0.80 (0.03)	0.89 (0.08)	0.81 (0.11)	0.69 (0.03)	0.55 (0.07)	0.95 (0.02)	0.62 (0.06)	0.49 (0.04)
Ethanol+water+MNA+SLS	0.53 (0.03)	0.65 (0.05)	0.87 (0.03)	0.87 (0.05)	0.68 (0.04)	0.70 (0.04)	0.69 (0.02)	0.77 (0.09)	0.56 (0.06)	0.57 (0.08)
Water	1.08 (0.04)	1.25 (0.02)	2.53 (0.04)	1.92 (0.08)	2.95 (0.06)	3.78 (0.03)	3.01 (0.04)	0.74 (0.02)	1.72 (0.11)	1.97 (0.09)
Water+MNA	1.08 (0.04)	1.22 (0.04)	1.70 (0.13)	1.97 (0.04)	2.99 (0.21)	3.25 (0.06)	2.51 (0.05)	1.57 (0.06)	1.50 (0.04)	2.18 (0.15)
Water+SLS	1.17 (0.03)	1.21 (0.02)	1.30 (0.09)	1.37 (0.04)	1.11 (0.07)	1.42 (0.03)	1.28 (0.02)	1.31 (0.03)	1.21 (0.02)	1.21 (0.07)
Water+MNA+SLS	1.02 (0.02)	1.11 (0.01)	1.34 (0.03)	1.24 (0.04)	1.22 (0.03)	1.29 (0.02)	1.08 (0.02)	1.15 (0.05)	1.18 (0.03)	1.17 (0.04)
Ethanol+PG	1.08 (0.08)	0.88 (0.05)	1.08 (0.02)	0.92 (0.07)	0.78 (0.03)	0.96 (0.05)	0.78 (0.05)	1.09 (0.04)	0.75 (0.09)	0.91 (0.12)
Ethanol+PG+MNA	0.92 (0.07)	0.79 (0.05)	0.96 (0.04)	1.39 (0.04)	1.03 (0.16)	0.85 (0.09)	0.88 (0.01)	1.01 (0.03)	0.95 (0.07)	0.85 (0.07)
Ethanol+PG+SLS	0.56 (0.06)	0.42 (0.04)	0.86 (0.02)	0.91 (0.09)	0.89 (0.04)	0.82 (0.05)	0.73 (0.06)	1.02 (0.09)	0.79 (0.04)	0.64 (0.04)
Ethanol+PG+MNA+SLS	0.58 (0.02)	0.58 (0.04)	0.80 (0.03)	0.86 (0.07)	0.87 (0.06)	0.89 (0.04)	0.66 (0.08)	0.92 (0.07)	0.85 (0.11)	0.75 (0.06)
PG	0.69 (0.10)	0.88 (0.03)	1.40 (0.06)	1.37 (0.07)	1.10 (0.05)	1.24 (0.03)	0.89 (0.05)	0.78 (0.05)	1.26 (0.09)	0.99 (0.16)
PG+MNA	0.94 (0.06)	0.74 (0.11)	1.28 (0.03)	1.24 (0.05)	1.40 (0.03)	1.31 (0.06)	0.85 (0.03)	1.31 (0.04)	0.99 (0.12)	1.20 (0.14)
PG+SLS	0.70 (0.07)	0.46 (0.05)	1.12 (0.04)	0.86 (0.05)	0.98 (0.02)	0.97 (0.04)	0.77 (0.11)	0.99 (0.06)	0.62 (0.05)	0.65 (0.04)
PG+MNA+SLS	0.67 (0.10)	0.54 (0.03)	1.06 (0.04)	0.80 (0.07)	1.03 (0.06)	0.86 (0.05)	0.74 (0.04)	0.91 (0.04)	0.75 (0.06)	0.80 (0.03)
Water+PG	0.80 (0.03)	0.78 (0.01)	1.75 (0.03)	1.29 (0.05)	1.42 (0.11)	2.09 (0.03)	1.58 (0.06)	1.00 (0.02)	0.75 (0.03)	0.95 (0.07)
Water+PG+MNA	0.73 (0.03)	0.63 (0.03)	1.84 (0.01)	1.17 (0.05)	2.02 (0.05)	2.17 (0.02)	1.49 (0.04)	0.94 (0.06)	0.77 (0.04)	0.97 (0.04)
Water+PG+SLS	0.58 (0.03)	0.50 (0.03)	0.92 (0.02)	0.93 (0.05)	0.81 (0.04)	0.72 (0.03)	0.72 (0.02)	1.04 (0.03)	0.66 (0.06)	0.61 (0.04)
Water+PG+MNA+SLS	0.65 (0.04)	0.66 (0.02)	1.12 (0.20)	0.80 (0.07)	0.89 (0.05)	1.10 (0.02)	0.76 (0.02)	0.90 (0.06)	0.67 (0.03)	0.71 (0.03)

PNP = *p*-Nitrophenol; PCP = pentachlorophenol; Mparathion = methyl parathion; PG = propylene glycol.

of the solutes are: 1.46 for phenol, 1.91 for *p*-nitrophenol, 2.18 for simazine, 2.61 for atrazine, 2.86 for methyl parathion, 2.93 for propazine, 3.83 for parathion, 4.09 for fenthion, 4.96 for chlorpyrifos and 5.12 for pentachlorophenol [7].

Cluster Analysis

Cluster analysis was conducted using the statistics toolbox of Matlab™ version 6.5.0.180913a release13 (The Mathworks Inc., Natick, Mass.). Two methods were used: K-means clustering and hierarchical clustering [8, 9].

To perform K-means clustering, variables were assigned to a pre-determined number of clusters based on the relatedness of the observations associated with each member of the cluster. Relatedness was determined through an iterative algorithm to minimize the sum of distances from each object to its cluster centroid. Mean silhouette values were used to determine the optimum number of clusters.

Hierarchical clustering created a multi-level binary cluster tree, which linked clusters formed at a lower level to form higher-level clusters. The Euclidian distances between pairs of variables in the data matrix were computed. Various indices of similarity and dissimilarity were used to link variables into a cluster tree including shortest distance, largest distance, average distance, centroid distance and incremental sum of squares. The relative efficiencies of the clustering solutions based on the similarity and dissimilarity indices were determined by calculating cophenetic correlation coefficients, which compared the cluster tree links with the distance vectors between pairs of data variables.

Results

Partitioning Data Structure

Stratum corneum/solvent partitioning results are summarized in table 2. The solvent systems were clustered based on their influence on the log stratum corneum/solvent partitioning (log P) values of 10 solutes (table 2) into hierarchical clusters (fig. 1) and K-means clusters (table 3). The optimum number of K-means clusters was 4, with a mean silhouette value of 0.6860 (table 3). The average distance provided the most efficient hierarchical clustering solution (fig. 1). The cophenetic correlation coefficients of the cluster trees were: 0.9311 for largest distance, 0.9620 for shortest distance, 0.9663 for average distance, 0.9658 for centroid distance and 0.9137 for incremental sum of squares. Hierarchical clustering and K-means clustering resulted in the same 4-cluster solution – except for solvent systems 5 (ethanol and water) and 6 (ethanol, water and MNA). They were grouped with the K-means cluster 1 (table 3), but with the hierarchical cluster 2. The hierarchical cluster 2 was similar to the K-means cluster 2.

Fig. 1. A hierarchical average distance cluster tree of 24 solvent systems based on the stratum corneum/solvent partitioning values of methyl parathion, ethyl parathion, atrazine, phenol, *p*-nitrophenol, pentachlorophenol, simazine, propazine, chlorpyrifos and fenthion. The solvent systems are: 1 – ethanol; 2 – ethanol and MNA; 3 – ethanol and SLS; 4 – ethanol, MNA and SLS; 5 – ethanol and water; 6 – ethanol, water and MNA; 7 – ethanol, water and SLS; 8 – ethanol, water, MNA and SLS; 9 – water; 10 – water and MNA; 11 – water and SLS; 12 – water, MNA and SLS; 13 – ethanol and propylene glycol; 14 – ethanol, propylene glycol and MNA; 15 – ethanol, propylene glycol and SLS; 16 – ethanol, propylene glycol, MNA and SLS; 17 – propylene glycol; 18 – propylene glycol and MNA; 19 – propylene glycol and SLS; 20 – propylene glycol, MNA and SLS; 21 – water and propylene glycol; 22 – water, propylene glycol and MNA; 23 – water, propylene glycol and SLS; 24 – water, propylene glycol, MNA and SLS.

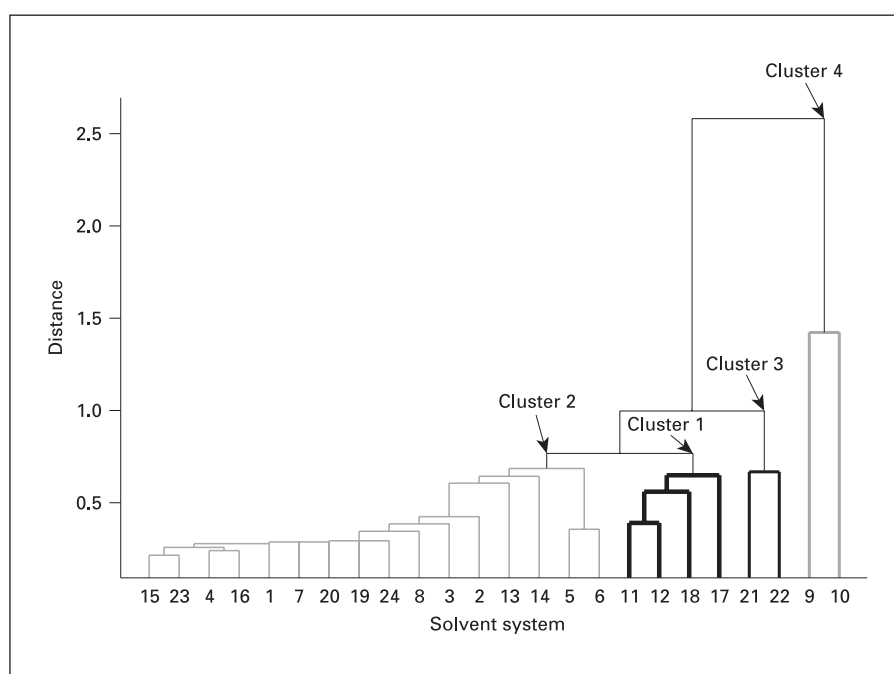


Table 3. K-means clustering based on stratum corneum/solvent partitioning

Solvent	Cluster
Ethanol + water	1
Ethanol + water + MNA	1
Water + SLS	1
Water + MNA + SLS	1
PG	1
PG + MNA	1
Ethanol	2
Ethanol + MNA	2
Ethanol + SLS	2
Ethanol + MNA + SLS	2
Ethanol + water + SLS	2
Ethanol + water + MNA + SLS	2
Ethanol + PG	2
Ethanol + PG + MNA	2
Ethanol + PG + SLS	2
Ethanol + PG + MNA + SLS	2
PG + SLS	2
PG + MNA + SLS	2
Water + PG + SLS	2
Water + PG + MNA + SLS	2
Water + PG	3
Water + PG + MNA	3
Water	4
Water + MNA	4

PG = Propylene glycol.

Permeability Data Structure

Permeability results are summarized in table 4. The solvent systems were clustered based on their influence on solute permeability values of 10 solutes (table 4) into hierarchical clusters (fig. 2) and K-means clusters (table 5). The optimum number of K-means clusters was 3, with a mean silhouette value of 0.7109 (table 5). The average distance provided the most efficient hierarchical clustering solution (fig. 2). The cophenetic correlation coefficients of the cluster trees were: 0.8889 for largest distance, 0.9265 for shortest distance, 0.9359 for average distance, 0.9356 for centroid distance and 0.8310 for incremental sum of squares. Water and water with MNA formed a separate cluster in hierarchical clustering, but formed part of the first K-means cluster (table 5; fig. 2). The second and third K-means clusters were preserved during hierarchical clustering.

Polarity Index

The polarity indexes for the solvent systems are summarized in table 1. The average polarity indexes for the hierarchical clusters and K-means clusters based on stratum corneum/solvent partitioning are summarized in table 6.

Fig. 2. A hierarchical average distance cluster tree of 24 solvent systems based on the skin permeability of methyl parathion, ethyl parathion, atrazine, phenol, *p*-nitrophenol, pentachlorophenol, simazine, propazine, chlorpyrifos and fenthion. The solvent systems are: 1 – ethanol; 2 – ethanol and MNA; 3 – ethanol and SLS; 4 – ethanol, MNA and SLS; 5 – ethanol and water; 6 – ethanol, water and MNA; 7 – ethanol, water and SLS; 8 – ethanol, water, MNA and SLS; 9 – water; 10 – water and MNA; 11 – water and SLS; 12 – water, MNA and SLS; 13 – ethanol and propylene glycol; 14 – ethanol, propylene glycol and MNA; 15 – ethanol, propylene glycol and SLS; 16 – ethanol, propylene glycol, MNA and SLS; 17 – propylene glycol; 18 – propylene glycol and MNA; 19 – propylene glycol and SLS; 20 – propylene glycol, MNA and SLS; 21 – water and propylene glycol; 22 – water, propylene glycol and MNA; 23 – water, propylene glycol and SLS; 24 – water, propylene glycol, MNA and SLS.

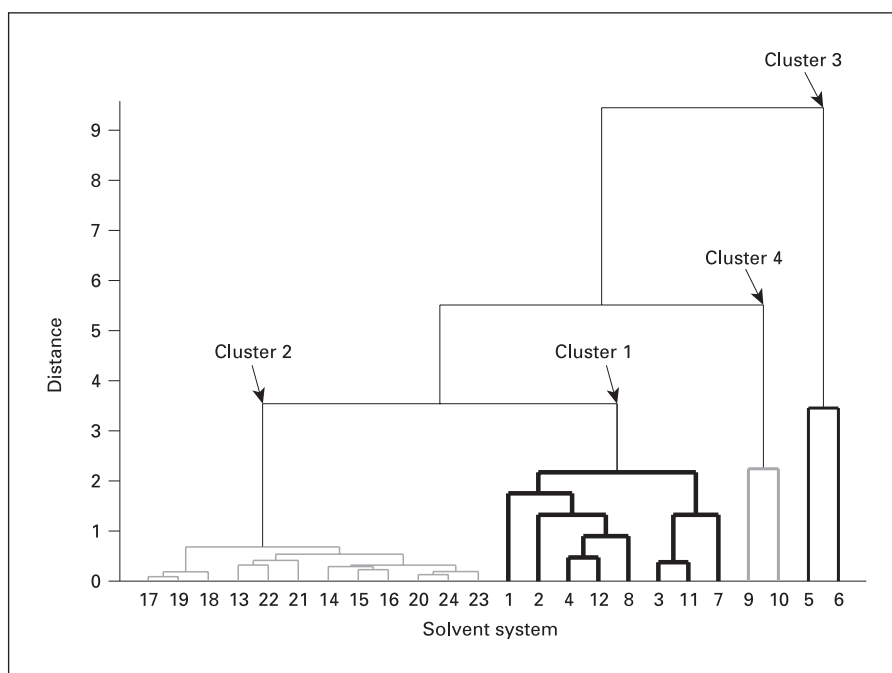


Table 4. Solute permeability (cm/hr $\times 10^{-3}$) followed by standard errors in brackets

	Phenol	PNP	PCP	Mparathion	Parathion	Chlorpyrifos	Fenthion	Simazine	Atrazine	Propazine
Ethanol	4.21 (0.29)	0.35 (0.02)	0.08 (0.02)	0.18 (0.02)	0.16 (0.03)	0.01 (0.00)	0.10 (0.01)	0.095 (0.01)	0.07 (0.00)	0.03 (0.01)
Ethanol+MNA	2.88 (0.32)	0.36 (0.03)	0.10 (0.02)	1.43 (0.47)	0.14 (0.01)	0.01 (0.00)	0.05 (0.00)	0.037 (0.00)	0.19 (0.05)	0.02 (0.00)
Ethanol+SLS	4.44 (0.24)	1.60 (0.07)	0.30 (0.08)	0.71 (0.05)	0.12 (0.01)	0.04 (0.00)	0.26 (0.04)	0.355 (0.03)	0.61 (0.03)	0.09 (0.01)
Ethanol+MNA+SLS	2.71 (0.42)	1.22 (0.13)	0.18 (0.03)	0.71 (0.11)	0.20 (0.02)	0.02 (0.00)	0.10 (0.01)	0.135 (0.00)	0.39 (0.04)	0.04 (0.01)
Ethanol+water	10.50 (0.41)	4.99 (0.22)	1.43 (0.27)	4.15 (0.32)	0.29 (0.02)	0.15 (0.03)	0.40 (0.04)	0.259 (0.03)	1.75 (0.12)	0.42 (0.04)
Ethanol+water+ MNA	8.00 (0.54)	6.26 (0.49)	0.32 (0.04)	3.08 (0.18)	0.37 (0.05)	0.11 (0.01)	0.18 (0.04)	0.081 (0.01)	0.74 (0.07)	0.06 (0.01)
Ethanol+water+ SLS	5.50 (0.06)	2.21 (0.06)	0.12 (0.04)	0.73 (0.04)	0.18 (0.01)	0.04 (0.01)	0.17 (0.02)	0.340 (0.05)	0.75 (0.07)	0.17 (0.01)
Ethanol+water+ MNA+SLS	3.36 (0.54)	1.17 (0.10)	0.06 (0.01)	0.45 (0.03)	0.28 (0.02)	0.04 (0.01)	0.02 (0.00)	0.293 (0.04)	0.38 (0.02)	0.09 (0.01)
Water	4.38 (0.19)	2.22 (0.34)	1.65 (0.22)	4.92 (0.63)	0.41 (0.05)	0.06 (0.02)	0.46 (0.01)	0.484 (0.06)	1.13 (0.22)	0.23 (0.01)
Water+MNA	3.56 (0.35)	3.12 (0.46)	0.65 (0.11)	3.81 (1.44)	1.12 (0.08)	0.02 (0.01)	0.36 (0.01)	0.218 (0.03)	0.45 (0.18)	0.05 (0.01)
Water+SLS	4.38 (0.23)	1.75 (0.09)	0.39 (0.04)	0.63 (0.07)	0.24 (0.04)	0.05 (0.01)	0.19 (0.03)	0.199 (0.04)	0.70 (0.12)	0.14 (0.03)
Water+MNA+SLS	2.75 (0.23)	1.21 (0.14)	0.27 (0.05)	0.94 (0.12)	0.46 (0.11)	0.04 (0.00)	0.06 (0.00)	0.172 (0.03)	0.37 (0.08)	0.03 (0.00)
Ethanol+PG	1.04 (0.12)	0.128 (0.01)	0.024 (0.00)	0.17 (0.02)	0.02 (0.00)	0.02 (0.00)	0.06 (0.01)	0.034 (0.01)	0.07 (0.00)	0.03 (0.00)
Ethanol+PG+MNA	0.73 (0.10)	0.146 (0.03)	0.007 (0.00)	0.27 (0.05)	0.03 (0.00)	0.02 (0.01)	0.02 (0.00)	0.049 (0.02)	0.08 (0.00)	0.03 (0.00)
Ethanol+PG+SLS	0.85 (0.05)	0.074 (0.01)	0.013 (0.00)	0.08 (0.01)	0.05 (0.01)	0.01 (0.00)	0.06 (0.01)	0.141 (0.03)	0.15 (0.02)	0.07 (0.01)
Ethanol+PG+MNA+SLS	0.74 (0.11)	0.067 (0.00)	0.010 (0.00)	0.15 (0.04)	0.06 (0.01)	0.01 (0.00)	0.01 (0.00)	0.231 (0.03)	0.15 (0.02)	0.07 (0.00)
PG	0.13 (0.01)	0.013 (0.00)	0.013 (0.00)	0.05 (0.01)	0.03 (0.00)	0.01 (0.00)	0.02 (0.00)	0.023 (0.00)	0.03 (0.02)	0.01 (0.00)
PG+MNA	0.22 (0.03)	0.039 (0.01)	0.015 (0.00)	0.17 (0.08)	0.06 (0.00)	0.01 (0.01)	0.01 (0.00)	0.034 (0.01)	0.06 (0.04)	0.01 (0.00)
PG+SLS	0.18 (0.02)	0.030 (0.01)	0.016 (0.00)	0.04 (0.01)	0.04 (0.02)	0.01 (0.00)	0.03 (0.00)	0.062 (0.04)	0.03 (0.00)	0.01 (0.00)
PG+MNA+SLS	0.50 (0.14)	0.026 (0.01)	0.010 (0.00)	0.06 (0.00)	0.06 (0.02)	0.02 (0.01)	0.02 (0.00)	0.165 (0.04)	0.13 (0.07)	0.01 (0.00)
Water+PG	1.32 (0.40)	0.152 (0.01)	0.091 (0.01)	0.23 (0.04)	0.03 (0.02)	0.02 (0.00)	0.09 (0.01)	0.022 (0.01)	0.12 (0.05)	0.02 (0.00)
Water+PG+MNA	0.90 (0.18)	0.324 (0.06)	0.020 (0.00)	0.20 (0.03)	0.03 (0.01)	0.04 (0.02)	0.07 (0.04)	0.044 (0.02)	0.22 (0.11)	0.01 (0.00)
Water+PG+SLS	0.61 (0.05)	0.049 (0.00)	0.020 (0.00)	0.08 (0.01)	0.04 (0.00)	0.04 (0.01)	0.04 (0.01)	0.048 (0.00)	0.10 (0.01)	0.05 (0.00)
Water+PG+MNA+SLS	0.56 (0.03)	0.060 (0.01)	0.010 (0.00)	0.12 (0.03)	0.11 (0.03)	0.01 (0.00)	0.01 (0.00)	0.157 (0.02)	0.16 (0.01)	0.03 (0.01)

PNP = *p*-Nitrophenol; PCP = pentachlorophenol; Mparathion = methyl parathion; PG = propylene glycol.

Table 5. K-means clustering based on permeability

Solvent	Cluster
Ethanol	1
Ethanol + MNA	1
Ethanol + SLS	1
Ethanol + MNA + SLS	1
Ethanol + water + SLS	1
Ethanol + water + MNA + SLS	1
Water	1
Water + MNA	1
Water + SLS	1
Water + MNA + SLS	1
Ethanol + PG	2
Ethanol + PG + MNA	2
Ethanol + PG + SLS	2
Ethanol+ PG + MNA + SLS	2
PG	2
PG + MNA	2
PG + SLS	2
PG + MNA + SLS	2
Water + PG	2
Water + PG + MNA	2
Water + PG + SLS	2
Water + PG + MNA + SLS	2
Ethanol + water	3
Ethanol + water + MNA	3

PG = Propylene glycol.

Table 6. The average polarity indexes and ranges of the hierarchical and K-means clusters based on stratum corneum/solvent partitioning

	Average polarity index	Range
Hierarchical clusters		
1	0.369	0.271–0.462
2	0.727	0.463–1.072
3	0.235	0.234–0.237
4	0.001	0.000–0.003
K-means clusters		
1	0.325	0.271–0.473
2	0.764	0.480–1.070
3	0.235	0.234–0.237
4	0.001	0.000–0.003

Discussion

A clustering structure based on solvent polarity emerged from the partitioning data (tables 3 and 6; fig. 1). Hierarchical cluster 1 may be described as mildly non-polar (average polarity index: 0.369), cluster 2 as substantially non-polar (average polarity index: 0.727), cluster 3 as mildly polar (average polarity index: 0.235) and cluster 4 as substantially polar (average polarity index: 0.001). K-means clusters showed similar polarity index values (table 6). The inter-molecular attraction between molecules of similar polarity is relatively higher when compared with the inter-molecular attraction between molecules of dissimilar polarity. Therefore, when other system conditions are equal, solute molecules in a solvent system of dissimilar polarity exist in a state of higher potential energy compared with solute molecules in a solvent system of similar polarity. Due to these effects of inter-molecular forces on enthalpy, energy equilibrium was reached when partitioning into the non-polar environment of the stratum corneum lipids of the relatively non-polar compounds was higher from polar than from non-polar solvents.

The addition of MNA to solvents did not alter partitioning – indicating that MNA had little effect on enthalpy. This was largely due to the low proportions (0.12–0.16% by mass) of the solvent systems consisting of MNA.

The addition of SLS caused solvent systems with relatively high proportions of water and no ethanol, which had low polarity index values indicating high polarity (table 1), to cluster with more non-polar solvents in the partitioning data (fig. 1), while the clustering behavior of non-polar solvents was unchanged. Partitioning from water of more polar solutes, such as phenol and *p*-nitrophenol, was not increased by the addition of SLS, while partitioning from water of more non-polar solutes, such as chlorpyrifos and pentachlorophenol, was increased (table 3). The detection of substantially polar solvent systems as a separate cluster from similar solvent systems with the addition of SLS indicated that, on average, the group of solutes partitioned similarly. However, correlation between the degree of solute non-polarity and the degree of change in partitioning supported the hypothesis that SLS forms micelles around non-polar molecules in water and reduces their potential energy in polar solvents [4, 10, 11]. These results also agree with previously published analyses, which indicated that partitioning into porcine stratum corneum from polar solvents is correlated with compound lipophilicity when using octanol/

water partitioning as a predictor of compound lipophilicity [10, 12].

The addition of MNA did not alter the permeability data structure. These results may not be relevant to the effects of MNA *in vivo* because MNA is a vasoconstrictor, but it indicates that MNA does not alter solute diffusivity in the skin.

Hierarchical clustering of the permeability data separated water from ethanol, water from water with SLS and water from ethanol with SLS (cluster 4, fig. 2), but the difference was not large enough to form a separate cluster using K-means clustering (table 5). The difference in clustering reflects differences in the efficiency of the two clustering methods. However, the separation detected in the hierarchical clusters based on permeability was consistent with the partitioning data structure and may be due to the influence of partitioning on permeability. Ethanol/water mixtures consistently formed a separate cluster due to higher permeability, which was not consistent with the clusters based on partitioning. Since the separation of ethanol/water mixtures cannot be explained based on partitioning, but consistently formed a separate cluster based on permeability (cluster 3, fig. 2), it suggests that this mixture significantly alters diffusivity. This result was consistent with findings from other studies, which reported enhanced dermal absorption when a mixture of ethanol and water was used as a solvent compared with water or ethanol alone [13–18].

Solvents containing propylene glycol formed a consistent cluster in the permeability data (cluster 2, fig. 2). This was due to consistently low solute permeability when compared with solvents without propylene glycol. Propylene glycol, with a vapor pressure of 0.129 mm Hg at 25°C, has a low rate of evaporation compared with water and ethanol, which have vapor pressures of 23.8 and 59.3 mm Hg at 25°C, respectively [7]. This supports the hypothesis that water and ethanol evaporation, when the skin surface is open to the atmosphere, causes solute super saturation if all or most of the solvent evaporates within the experimental period. Super saturation provides a high solute concentration gradient across the skin that accelerates solute absorption – an effect that would be absent from experiments using propylene glycol as the solvent due to the low volatility of propylene glycol. Super saturation could also explain the significance of Henry's law constant in hybrid quantitative structure permeation relationship models of permeability, which take solvent mixture effects into account. This is due to the influence of volatility on the value of Henry's law, which is defined as vapor pressure divided by water solubility [3].

Inconsistencies between the partitioning data structure and the permeability data structure suggested that the degree of solute partitioning into the skin does not predict the rate of solute movement through the skin. Since permeability incorporates both partitioning and rate of movement, permeability cannot be derived from partitioning data alone. It follows that predictive models of dermal absorption over limited periods of time that include partitioning and rate of movement terms should perform better than models that are based solely on partitioning. Solutes partitioned into the stratum corneum may be absorbed over long periods of time in spite of low diffusivity, while low diffusivity can have a more limiting influence on total absorption over the time span of an 8-hour experiment. Therefore, models that predict partitioning could be more successful for predicting total absorption over infinite time, but such models may not be clinically relevant.

We concluded that the determining influence of solvent polarity on the partitioning data structure supported the hypothesis that solvent polarity drives the partitioning of non-polar solutes. Solvent polarity did not consistently predict permeability because solvent effects on diffusivity masked the effects of partitioning on permeability. The consistent reduction in permeability associated with the inclusion of propylene glycol, which has a low volatility compared with water and ethanol, in the solvent system supports the hypothesis that super saturation due to solvent evaporation has a marked effect on permeability. These results demonstrated the potential of using cluster analysis of large datasets to identify consistent solvent and chemical mixture effects on permeability related to identifiable solvent characteristics. Expansion of such datasets should be balanced by including compounds and chemical mixtures representing a range of physical-chemical characteristics. This approach does not allow exact predictions of permeability, but it could be valuable when novel chemical mixtures are assessed. In a practical sense, it could enable improved permeability estimation for the purposes of risk assessment of chemical exposure and the potential for pharmaceutical drug absorption from complex chemical mixtures.

Acknowledgements

This work was partially supported by NIOSH OH-07555. We thank the staff of the Center for Chemical Toxicology Research and Pharmacokinetics at North Carolina State University for the technical support.

References

- 1 Scheuplein RJ, Blank IH: Permeability of the skin. *Physiol Rev* 1971;51:702–747.
- 2 Potts RO, Guy RH: A predictive algorithm for skin permeability: the effects of molecular size and hydrogen bond activity. *Pharm Res* 1995; 12:1628–1633.
- 3 Riviere JE, Brooks JD: Predicting skin permeability from complex chemical mixtures. *Toxicol Appl Pharmacol* 2005;208:99–110.
- 4 Baynes RE, Brooks JD, Mumtaz M, Riviere JE: Effect of chemical interactions in pentachlorophenol mixtures on skin and membrane transport. *Toxicol Sci* 2002;69:295–305.
- 5 Chang SK, Riviere JE: Percutaneous absorption of parathion in vitro in porcine skin: effects of dose, temperature, humidity, and perfusate composition on absorptive flux. *Fundam Appl Toxicol* 1991;17:494–504.
- 6 Bronaugh RL, Stewart RF: Methods for in vitro percutaneous absorption studies V: permeation through damaged skin. *J Pharm Sci* 1985; 74:1062–1066.
- 7 Interactive PhysProp Database Demo: Syracuse Research Corporation, 2005. Accessed at <http://www.syrres.com/esc/physdemo.htm>.
- 8 Jain AK, Dubes RC: Algorithms for Clustering Data. Upper Saddle River, Prentice-Hall, 1988.
- 9 Duda OR, Hart PE, Stork DG: Pattern Classification, ed 2. New York, Wiley-Interscience, 2000.
- 10 van der Merwe D, Riviere JE: Effect of vehicles and sodium lauryl sulphate on xenobiotic permeability and stratum corneum partitioning in porcine skin. *Toxicology* 2005;206:325–335.
- 11 Shokri J, Nokhodchi A, Dashbolaghi A, Hassan-Zadeh D, Ghafourian T, Barzegar Jalali M: The effect of surfactants on the skin penetration of diazepam. *Int J Pharm* 2001;228: 99–107.
- 12 van der Merwe D, Riviere JE: Comparative studies on the effects of water, ethanol and water/ethanol mixtures on chemical partitioning into porcine stratum corneum and silastic membrane. *Toxicol In Vitro* 2005;19:69–77.
- 13 Panchagnula R, Salve PS, Thomas NS, Jain AK, Ramarao P: Transdermal delivery of naloxone: effect of water, propylene glycol, ethanol and their binary combinations on permeation through rat skin. *Int J Pharm* 2001;219: 95–105.
- 14 Kim DD, Kim JL, Chien YW: Mutual hairless rat skin permeation-enhancing effect of ethanol/water system and oleic acid. *J Pharm Sci* 1996;85:1191–1195.
- 15 Berner B, Mazzenga GC, Otte JH, Steffens RJ, Juang RH, Ebert CD: Ethanol: water mutually enhanced transdermal therapeutic system II: skin permeation of ethanol and nitroglycerin. *J Pharm Sci* 1989;78:402–407.
- 16 Kurihara-Bergstrom T, Knutson K, DeNoble LJ, Goates CY: Percutaneous absorption enhancement of an ionic molecule by ethanol-water systems in human skin. *Pharm Res* 1990; 7:762–766.
- 17 Megrab NA, Williams AC, Barry BW: Oestradiol permeation across human skin, silastic and snake skin membranes: the effects of ethanol/water co-solvent systems. *Int J Pharm* 1995;116:101–112.
- 18 Levang AK, Zhao K, Singh J: Effect of ethanol/propylene glycol on the in vitro percutaneous absorption of aspirin, biophysical changes and macroscopic barrier properties of the skin. *Int J Pharm* 1999;181:255–263.

Reproduced with permission of the copyright owner. Further reproduction prohibited without permission.